Malaysian Journal of Mathematical Sciences 16(2): 257–272 (2022)
https://doi.org/10.47836/mjms.16.2.06

Malaysian Journal of Mathematical Sciences

Journal homepage: https://einspem.upm.edu.my/journal

Hybrid Nanofluid Flow in a Porous Medium with Second-Order Velocity Slip, Suction and Heat Absorption

Bakar, S. A.*[1], Arifin, N. M.[1,2], Bachok, N.[1,2], and Ali, F. M.[1,2]

[1]*Institute for Mathematical Research, Universiti Putra Malaysia, Malaysia*
[2]*Department of Mathematics & Statistics, Faculty of Science, Universiti Putra Malaysia, Malaysia*

E-mail: shahirah.bakar@upm.edu.my
**Corresponding author*

Received: 18 June 2021
Accepted: 19 January 2022

Abstract

The foremost objective of this study is to reflect the behaviour of hybrid nanofluid towards a permeable porous medium, with consideration of second-order velocity slip and heat absorption impacts on the fluid flow. Two distinct fluids of copper (Cu) and aluminium oxide (Al_2O_3) are reviewed in this study to work out as a hybrid nanofluid flow. The equations of boundary layer flow in the form of partial differential equations are reduced to a system of ODEs by conducting a similarity transformation technique, and the findings that obtained from this study are presented in the respective tables and figures. The effects of involving parameters such as suction, porous medium permeability, heat absorption and second order velocity slip are perceived, as well as our intention in observing the impact of traditional nanofluid and hybrid nanofluid on the fluid flow. Our findings revealed that the hybrid Cu-Al_2O_3/water nanofluid performs well on the fluid flow behaviour against the mono Al_2O_3/water nanofluid. Moreover, the participating parameters of porous medium permeability, suction and nanoparticle volume fraction are said to improve the boundary layer thickness, while second-order velocity slip parameter is deemed to decay the fluid flow.

Keywords: hybrid nanofluid; porous medium; free convection; second-order velocity slip; suction.

1 Introduction

Nowadays, various ways of enhancing heat transfer such as changing boundary conditions, flow geometry or thermal conductivity of the fluid are proposed. However, the large size of the suspended particles may result in erosion and microchannels logging. Hence, the smaller sized particles, or nanoparticles, are proposed as in the case of nanofluids. Nanofluids are used to increase the effectiveness of thermal conductivity on base fluid like water, ethylene glycol, kerosene and others. Copper, oxides, carbides, nitrides, and materials that are chemically stable are among of those generated in nanoparticles. The materials in nanofluids which are in nanometer size possess unique chemical and physical properties. They can flow through micro-channels smoothly without clogging because of their sufficiently small to similar behave as liquid molecules. This fact of nanofluids has attracted much research in this area of heat transfer investigations. Choi and Eastman [3] showed that a small number of nanoparticles added into the system can double up the performance of thermal conductivity in the fluids. Recently, an extensive combination of two nanoparticles was carried out by many researchers due to its great significance impact in various industries, including generator cooling management, microfluidics, naval structures, medical lubrication, and solar heating. The combination of these two nanoparticles conjoint a technique known as 'hybrid nanofluid'. In modern industries applications, Nieh et al. [17] used TiO_2 and Al_2O_3 in an air-cooled radiator to increase the heat dissipation, while Hung et al. [11] described the influence of hybrid nanoliquids in an air-cooled heat exchanger (ACHE), see Figure 1.

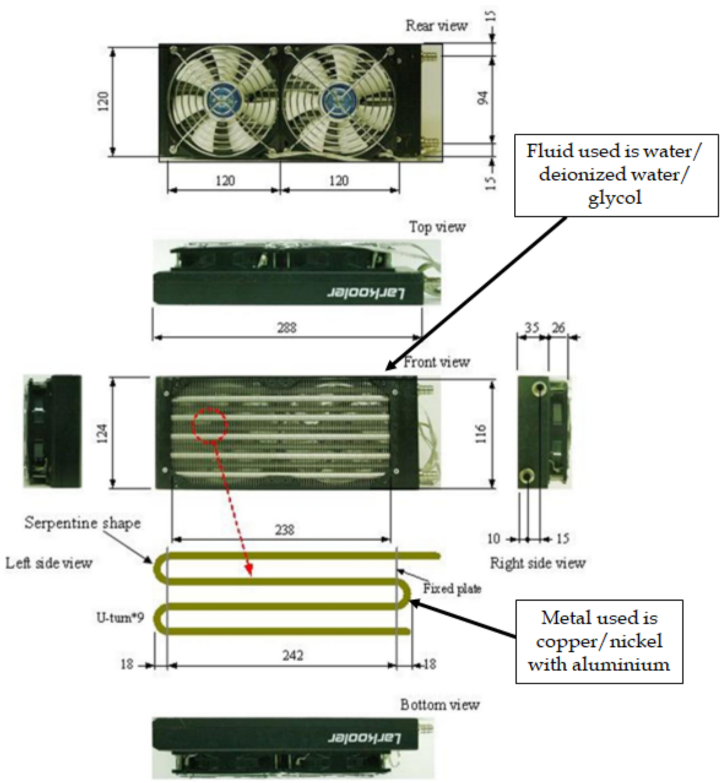

Figure 1: Liquid CPU cooler heat exchanger with hybrid nanoliquids, see Hung et al. [11].

The reason of this combination is due to the weakness that each nanoparticle should bares. For instance, aluminium oxide (Al_2O_3) has beneficial features like good chemical inertness and stability but exhibits lower thermal conductivity ($k = 40$). In a contrary, other metallic nanoparticles such as copper (Cu) and silver (Ag) are benefited with great thermal conductivities (Cu with $k = 401$, Ag with $k = 429$). Due to this, the bad condition of Al_2O_3 can stabilize when the combination of Cu and Al_2O_3; or Ag and Al_2O_3; is carried out. In a bigger scope, the vulnerable side of one material can be balance out by a properly composition of two nanomaterials, and thus enhance the positive features of each other. Hence, this combination of hybrid nanofluid was initiated to perform better due to its physical properties, and yet able to minimize the production cost, as explained by Ghadikolaei et al. [8]. Many previous reports and experimental studies claimed remarkable results based on the hybrid nanofluid performances, such as by Suresh et al. [19], where they elaborated the hybrid Cu-Al_2O_3/water nanofluid and its thermophysical properties by using two step method. Their proposed study created a new nanomaterial concept design, and thus positively performed on the properties of mechanical and thermal. Devi and Devi [6] performed a study on the effect of suction in Cu-Al_2O_3/water over a stretching sheet with hydromagnetic. From this study, they intended to conclude that the fluid flow is consistent and improves the rate of heat transfer by considering hybrid nanofluid under the magnetic field environment. Usman et al. [21] examined a study of nonlinear radiation and variable thermal conductivity on a permeable surface of hybrid Cu-Al_2O_3/water nanofluid, where they finalised that the impact of hybrid Cu-Al_2O_3 nanofluid gives more dominance on velocity and temperature profiles as compared to single Al_2O_3/water nanoparticle and single Cu/water nanoparticle. Another work on hybrid nanofluid flow was successfully reported by Chu et al. [4] and their study concluded that the nanoparticle fraction uplifted the velocity in asisting flow while decelerating in opposing flow. Ezhil et al. [7] then reported that the hybrid nanofluid is best to use as a heater with growing magnetic parameter, while Yan et al. [25] explained the existence of dual solutions is possessed, but do not exist beyond the critical value of suction and magnetic parameters at the same time.

On the other hand, the concept of hybrid nanofluid flow in a porous medium attracts much considerable interest due to its application scenarios in heat transfer theory and thus, since the porosity structure is encountered in many conditions and applications, including in technology and nature. The significance of hybrid nanofluid in porous channel has been considered by Das et al. [5] with consideration of MHD and entropy generation. The result of theirs concluded the hybrid nanofluid possesses a positive performance through thermal conductivities in the rate of heat transfer augmentation. Waini et al. [23] analyzed the mixed convection of a hybrid nanofluid flow embedded in a porous medium past a vertical surface, and they concluded the appearance of nanoparticle volume parameter enhances the rate of heat transfer. Lund et al. [15] then confirmed that by comparison of hybrid nanofluid, viscous fluid and mono-nanofluid with a porous medium, hybrid nanofluid showed the most efficient method in cooling processes due to hybrid nanoparticle volume fraction of copper-alumina possessed the highest boundary layer separation and thus elevate the fluid flow. Haider et al. [10] then scrutinised the conclusion of porosity parameter does the elevation of skin friction coefficient. Jamshed et al. [13] later examined a silver-copper nanoparticle dispersed on non-Newtonian engine oil in a Williamson porous medium with shape factor over a stretching surface, while Venkateswarlu and Narayana [22] explored a hybrid nanofluid flow over a porous stretching sheet due to temperature-dependent viscosity and viscous dissipation.

The significance of permeable surface (suction/injection) in a fluid flow is to affect and change the heat transfer rate from the fluid surface. Al-Sanea [2] explained that the suction is a method of physically increase the rate of heat transfer and skin friction coefficient, while injection tends to decrease both. The appearance of suction/injection through the surface, such as in electronic or engine cooling system, is applied widely in various engineering and technical applications. A suction machine, for instance, is also known as aspirator and presented widely as a medical device that is primarily used for removing obstructions such as blood, mucus or saliva. This characteristic of suction/injection that practically essential attracted researchers and academicians to work the hybrid nanofluid flow over a permeable surface. The study of hybrid nanofluid flow over a permeable stretching/shrinking surface with MHD and radiation is successfully scrutinized by Yashkun et al. [26], while Abu Bakar et al. [1] examined the flow of hybrid nanofluid past a permeable shrinking sheet in a Darcy-Forchheimer porous medium. Recently, Gokulavani et al. [9] explained in their study that suction possessed efficient rate of heat transfer compared to injection. The Nusselt number is also reported to be increase by 2% with the addition of nanofluidic volume particle.

In view of the aforementioned literatures, we intend to analyze the hybrid nanofluids of copper (Cu)/water and aluminium oxide (Al_2O_3)/water flow embedded in a porous medium with the appearance of suction, second-order velocity slip and internal heat absorption. Our mathematical models in this recent work are thoroughly under the assumption by Manjunatha et al. [16] where we extend the flow with conditions of second-order velocity slip and suction on the boundary limitations. In addition, we associated with three research questions that arise throughout this study:

1. Which model of nanoparticle between mono and hybrid that achieves better behaviour on the fluid flow?
2. Does velocity slip parameters d_1 and d_2 improve or decay the thermal transmittance and fluid flow?
3. Does suction parameter S improve or decay the thermal transmittance and fluid flow?

Hence, this current research will provide the answers and outcomes on the three research questions. A system of ordinary differential equations ODEs is deducted from a governing set of partial differential equations PDEs to work as a current mathematical model with the consideration of similarity transformation technique, and the results are solved numerically with the aid of shooting technique via Maple software. In the following sections, the model is formulated, analyzed and numerically solved. The results of all profiles are graphically presented and thoroughly discussed.

2 Current Mathematical Formulation

2.1 Modelling of the Fluid Flow

Let us consider a theoretical analysis on the steady and incompressible permeability of a porous medium and second-order velocity slip boundary layer through a water grounded by Cu-Al_2O_3 nanoparticles in the presence of internal heat absorption and permeable surface. We employed the Boussinesq approximation and the local thermal equilibrium with homogeneity in the porous medium are presumed. Figure 2 presented the geometry sketch of the hybrid nanofluid flow with permeable and velocity slip surrounded on the boundary limitations. With foregoing assumptions, the continuity, momentum and energy equations of hybrid nanofluid flow are written as

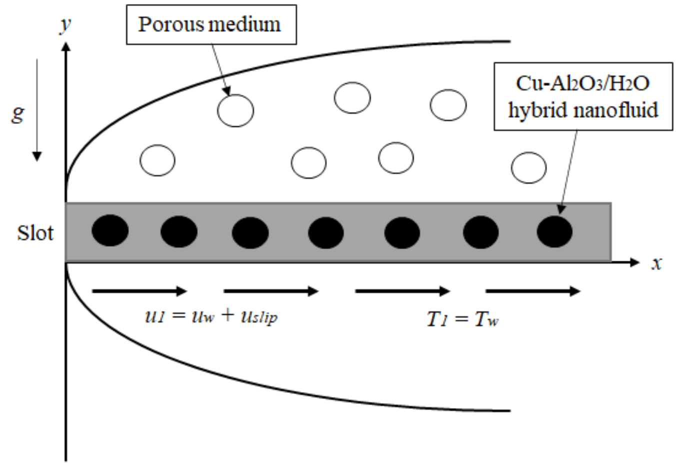

Figure 2: Flow geometry of the current system.

$$\frac{\partial u_1}{\partial x}+\frac{\partial v_1}{\partial y}=0, \tag{1}$$

$$\rho_{hnf}\left(u_1\frac{\partial u_1}{\partial x}+v_1\frac{\partial u_1}{\partial y}\right)=\mu_{hnf}\left(\frac{\partial^2 u_1}{\partial y^2}-\frac{u_1}{\kappa}\right)+\frac{\partial u_1}{\partial y}\frac{\partial \mu_{hnf}}{\partial y}, \tag{2}$$

$$(\rho C_p)_{hnf}\left(u_1\frac{\partial T_1}{\partial x}+v_1\frac{\partial T_1}{\partial y}\right)=k_{hnf}\frac{\partial^2 T_1}{\partial y^2}+Q_1(T_1-T_\infty). \tag{3}$$

The appropriate boundary conditions are as follows:

$$\begin{cases} u_1=u_w+u_{slip},\ v_1=v_w,\ T_1=T_w \ \text{ at } \ y=0, \\ u_1\to 0, v_1\to 0, T_1\to T_\infty \ \text{ as } \ y\to\infty. \end{cases} \tag{4}$$

Here the velocity components of hybrid nanofluid are presented by u_1 and v_1 along the $x-$ and $y-$directions, respectively, while ρ, μ, C_p, k represent density, dynamic viscosity, thermal capacity, thermal conductivity, with *hnf* notes the hybrid nanoparticles, respectively, κ is porous medium permeability, the rate of heat generation/absorption denoted by Q_1 with $Q_1>0$ beings heat generation and $Q_1<0$ is heat absorption, T_1 is the temperature of hybrid nanofluid, T_∞ is the ambient of hybrid nanofluid temperature, as well as the velocity slip factor and velocity of suction are represented by u_w and v_w, accordingly. The respective hybrid nanofluid thermophysical properties are listed in Table 1, while the thermophysical properties values of nanoparticles are exhibited in Table 2.

Table 1: Thermophysical models of hybrid nanofluids.

Properties	**Hybrid Nanofluid**
Density	$\rho_{hnf} = (1-\phi_2)[(1-\phi_1)\rho_f + \phi_1\rho_{s1}] + \phi_2\rho_{s2}$
Dynamic viscosity	$\mu_{hnf} = \dfrac{\mu_f}{(1-\phi_1)^{2.5}(1-\phi_2)^{2.5}}$
Heat capacity	$(\rho C_p)_{hnf} = (1-\phi_2)[(1-\phi_1)(\rho C_p)_f + \phi_1(\rho C_p)_{s1}] + \phi_2(\rho C_p)_{s2}$
Thermal conductivity	$\dfrac{k_{hnf}}{k_{nf}} = \dfrac{k_{s2}+2k_{nf}-2\phi_2(k_{nf}-k_{s2})}{k_{s2}+2k_{nf}+\phi_2(k_{nf}-k_{s2})}$ where $\dfrac{k_{nf}}{k_f} = \dfrac{k_{s1}+2k_f-2\phi_1(k_f-k_{s1})}{k_{s1}+2k_f+\phi_1(k_f-k_{s1})}$

Table 2: Value of thermophysical properties for H_2O and corresponding nanoparticles.

Physical Properties	**Density, ρ**	**Thermal capacity, C_p**	**Thermal conductivity, *k***
H_2O	997.1	4179	0.613
Cu	8933	385	401
Al_2O_3	3970	765	40

As suggested by Wu [24] and Ibrahim [12], the slip velocity u_{slip} is introduced as

$$u_{slip} = \alpha\frac{\partial u_1}{\partial y} + \beta\frac{\partial^2 u_1}{\partial y^2}, \tag{5}$$

where α and β are constants. In order to reduce the PDEs in Equations (1)-(3), the following dimensionless variables are instigated by

$$u_1 = \frac{u_0 x}{1-\xi}f'(\eta),\ v_1 = -\sqrt{\frac{u_0\nu_f}{1-\xi}}f(\eta),\ \theta(\eta) = \frac{T_1 - T_\infty}{T_w - T_\infty}, \tag{6}$$

where η is similarity variable and defined as $\eta = y\sqrt{\dfrac{u_0}{\nu_f(1-\xi)}}$. The dimensionless variables in Equation (6), together with similarity variable η, are proposed based on the standard application for the reduction of similarity transformation as in Equations (1)-(3).

Due to this, Equation (1) is clearly satisfied, and Equations (2)-(3) can reduced to

$$f''' - Kf' - A_1(f')^2 + A_1 ff'' = 0, \tag{7}$$

$$\frac{k_{hnf}}{k_f}\theta'' + A_2 Pr f\theta' + PrG\theta = 0, \tag{8}$$

and the boundary limitation as in Equation (4) is imposed to

$$\begin{cases} f(0) = S,\ f'(0) = 1 + d_1 f''(0) + d_2 f'''(0),\ \theta(0) = 1, \\ f'(\infty) \to 0,\ \theta(\infty) \to 0, \end{cases} \tag{9}$$

where K is porous medium permeability parameter, Pr is the local Prandtl number, G is heat absorption parameter, suction parameter is S, while the first-order and second-order velocity slips parameters are represented by d_1 and d_2, accordingly, which are defined as

$$\begin{cases} K = \dfrac{\nu_f(1-\xi)}{u_0\kappa},\ Pr = \dfrac{\nu_f(\rho C_p)_f}{k_f},\ G = \dfrac{Q_1(1-\xi)}{u_0(\rho C_p)_f}, \\ S = -\dfrac{\nu_w}{1-\xi},\ d_1 = \alpha\sqrt{\dfrac{u_0}{\nu_f}},\ d_2 = \beta\sqrt{\dfrac{u_0}{\nu_f}}, \end{cases} \tag{10}$$

and the notation of A_1 and A_2 are denoted as

$$\begin{cases} A_1 = \dfrac{1}{(1-\phi_1)^{2.5}(1-\phi_2)^{2.5}\left\{(1-\phi_2)\left[(1-\phi_1)+\phi_1\left(\dfrac{\rho_{s1}}{\rho_f}\right)\right]+\phi_2\left(\dfrac{\rho_{s2}}{\rho_f}\right)\right\}}, \\ A_2 = \left\{(1-\phi_2)\left[(1-\phi_1)+\phi_1\left(\dfrac{(\rho C_p)_{s1}}{(\rho C_p)_f}\right)\right]+\phi_2\left(\dfrac{(\rho C_p)_{s2}}{(\rho C_p)_f}\right)\right\}. \end{cases} \tag{11}$$

Here ϕ is volume particle parameter, where ϕ_1 being nanoparticle parameter for Cu and ϕ_2 being nanoparticle parameter for Al_2O_3.

2.2 Important Physical Quantities

The skin friction factor C_f and the specific Nusselt number Nu_x are the substantial important quantities regarding on the heat transfer, which are obtained as

$$\begin{cases} C_f = \dfrac{\tau_w}{\rho_f u_0^2}, \\ Nu_x = \dfrac{xq_w}{k_f(T_w - T_\infty)}, \end{cases} \tag{12}$$

where the surface shear stress along the sheet is τ_w and the surface heat flux at the wall is q_w, which are given by

$$\begin{cases} \tau_w = \left(\dfrac{\partial u_1}{\partial y}\right)_{y=0}\mu_{hnf}, \\ q_w = -\left(\dfrac{\partial T_1}{\partial y}\right)_{y=0}k_{hnf}. \end{cases} \tag{13}$$

Implementing Equation (6) in Equation (12), we finally have

$$\begin{cases} C_f Re_x^{1/2} = \dfrac{1}{(1-\phi_1)^{2.5}(1-\phi_2)^{2.5}}f''(0), \\ Nu_x Re_x^{-1/2} = -\dfrac{k_{hnf}}{k_f}\theta'(0), \end{cases} \tag{14}$$

where the local Reynolds number is denoted as $Re_x = \dfrac{u_w x}{\nu_f}$.

3 Results and Discussions

3.1 Comparative Analysis

The flow of hybrid Cu-Al_2O_3/H_2O nanofluid and free convection in a permeable non-Darcy porous medium with internal heat absorption and second order velocity slip is numerically studied in this current problem. The number of nanoparticles in this study is assumed to be 5% (volume of 0.05) for Cu, 2% (volume of 0.02) for Al_2O_3 and 93% (volume of 0.93) for H_2O, in order to prepare the hybrid nanofluid form. To validate the accuracy of our current findings, Table 3 listed the comparison of skin friction coefficient analysis $C_f Re_x^{1/2}$ between our present result, Oyelakin et al. [18] and Tulu and Ibrahim [20]; while Table 4 presented the comparison of temperature gradient analysis $Nu_x Re_x^{-1/2}$ between Manjunatha et al. [16], Khan and Pop [14] and present finding. Other parameters, including volume particle parameter, are fixed to be 0% in order to perceive the comparison. Based on these comparisons, we discovered a good consensus throughout the numerical findings and this leads confidence in the numerical results to be investigated subsequently.

Table 3: The similarities of $C_f\sqrt{Re_x}$ against first-order velocity slip parameter d_1.

d_1	$C_f\sqrt{Re_x}$		
	Present outcome	**Oyelakin et al. [18]**	**Tulu and Ibrahim [20]**
0.0	1.000022	1.0000	1.0000
0.1	0.872108	0.8721	0.8721
0.3	0.701579	0.7764	0.7764
0.5	0.591231	0.5912	0.5912
2.0	0.283930	0.2840	0.2840
5.0	0.144895	0.1447	0.1448
10.0	0.0018294	0.0809	0.0813

Table 4: The similarities of $Nu_x Re_x^{-1/2}$ against Prandtl number *Pr*.

Pr	$Nu_x Re_x^{-1/2}$		
	Present outcome	**Khan and Pop [14]**	**Manjunatha et al. [16]**
0.7	0.453980	0.4539	–
2.0	0.911344	0.9113	0.9114
7.0	1.895395	1.8954	1.8954
20.0	3.353897	3.3539	3.3539
70.0	6.462194	6.4621	–

Further, the comparisons of skin friction coefficient $C_f\sqrt{Re_x}$ and the local Nusselt number $Nu_x Re_x^{-1/2}$ between mono Al_2O_3/water nanofluid ($\phi_1 = 0\%, \phi_2 = 2\%$) and hybrid Cu-$Al_2O_3/H_2O$ nanofluid ($\phi_1 = 5\%, \phi_2 = 2\%$) are displayed in Figures 3 and 4, respectively. The numbers of $C_f\sqrt{Re_x}$ and $Nu_x Re_x^{-1/2}$ tend to enhance gradually with the increasing amount of suction parameter *S* and first-order velocity slip d_1. In addition, we observe that the hybrid Cu-Al_2O_3/water nanofluid impact on the boundary layer thickness tends to show a promising improvement rather than the traditional Al_2O_3/water nanoparticle. This positive improvement of fluid behaviour can be related to numerous works and reports that claiming the benefit of hybrid nanofluid in improving heat transfer rate, as emphasized by Ghadikolaei et al. [8]. Hence, we are positively agreed that the form of hybrid nanofluid can display a greater performance in the fluid flow rather than traditional nanofluid.

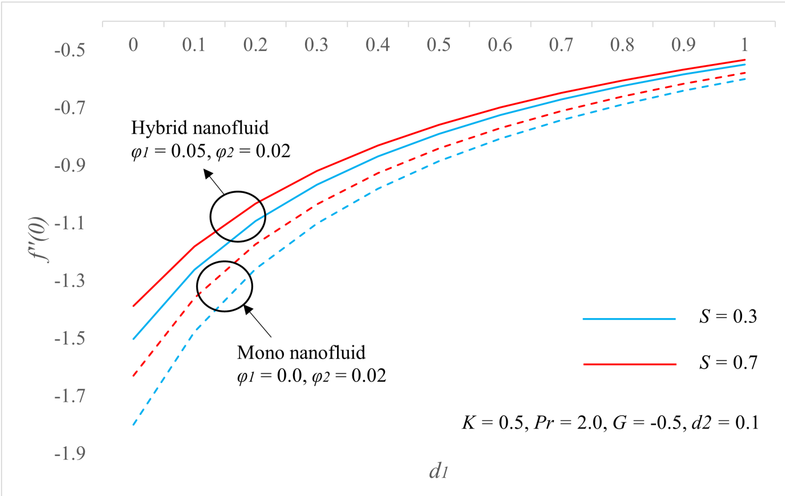

Figure 3: Skin friction coefficient $C_f\sqrt{Re_x}$ against d_1 when $S = 0.3$ and $S = 0.7$.

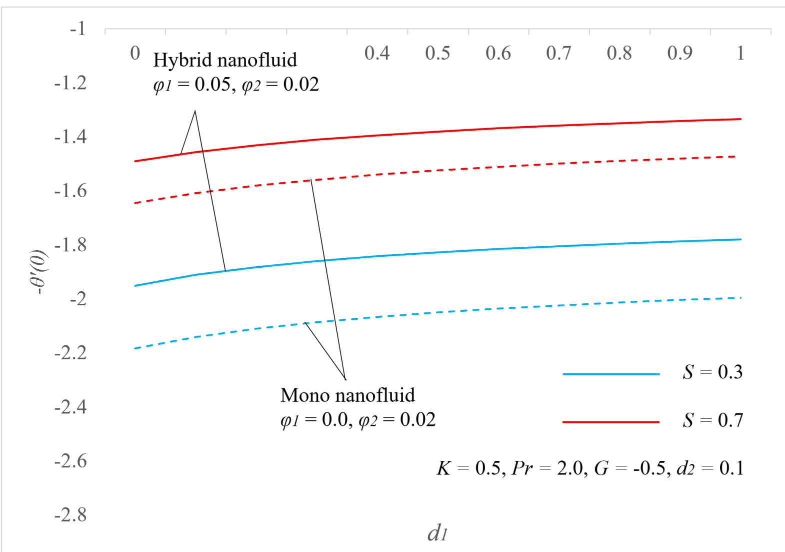

Figure 4: Local heat transfer rate $Nu_x Re_x^{-1/2}$ against d_1 when $S = 0.3$ and $S = 0.7$.

3.2 Physical Description of Fluid Profiles

The behaviour of velocity profiles $f'(\eta)$ with second-order velocity slip parameter d_2 is displayed in Figure 5 where we observed the decreasing pattern of the boundary layer flow. Tulu and Ibrahim [20] explained that the parameter of d_2 improves the fluid motion resistance, which decrease the field of fluid flow and the hybrid nanofluid boundary layer thickness. Hence, the consideration of second-order velocity slip condition in the flow of hybrid nanofluid especially in the nanotechnology sectors should not be neglected and derelict as it can plays a very important subject in the respective field. Figure 6 plotted the profiles of hybrid nanofluid velocity $f'(\eta)$ versus several numbers of porous medium permeability parameter K, where we confirmed that the thickness of boundary layer is improving against the additional number of K. The reason behind this increasing pattern is due to more fluid speed is scrutinized in entire fluid region when additional permeability is applied. Further, Figure 7 illustrated the temperature profiles $\theta\eta$ against several numbers of heat absorption parameter G. The thermal boundary layer thickness enhances when G increases, due to more heat in the fluid is produced and this causes a stronger boundary layer thickness and higher temperature, simultaneously.

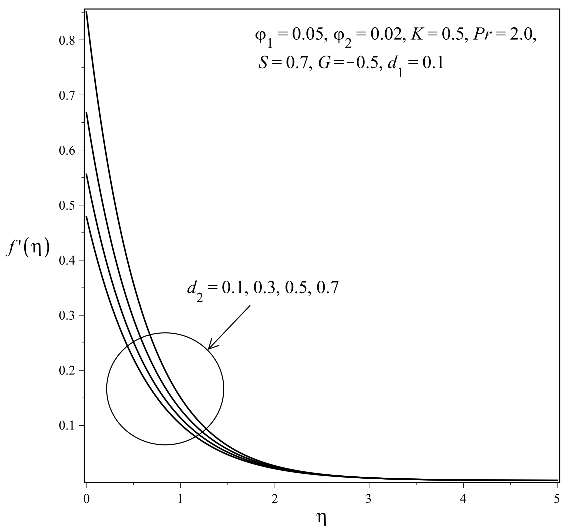

Figure 5: Velocity profiles $f'(\eta)$ with second-order velocity slip parameter d_2.

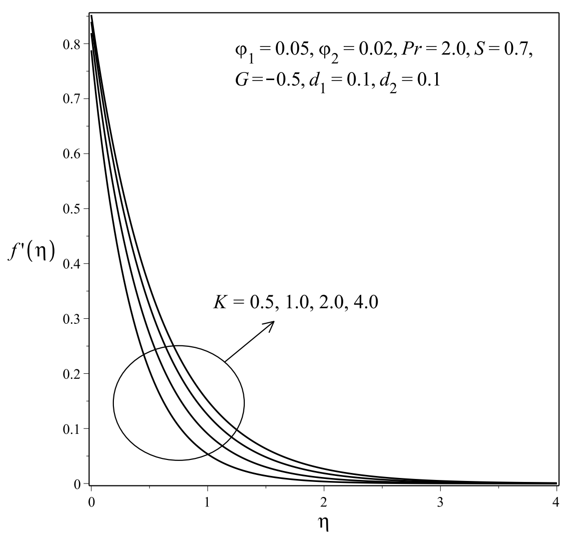

Figure 6: Velocity profiles $f'(\eta)$ with porous medium permeability K.

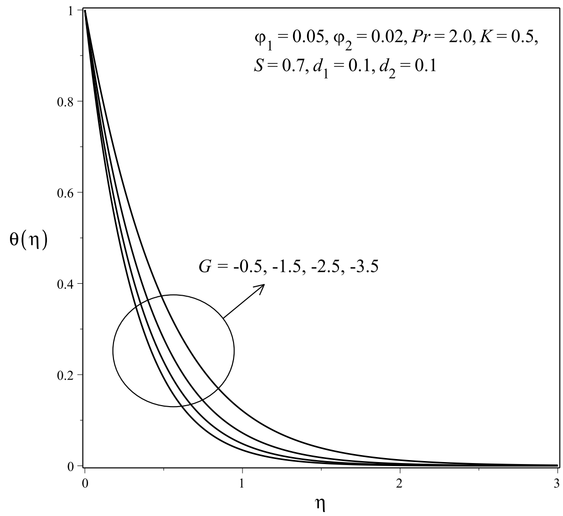

Figure 7: Temperature profiles $\theta(\eta)$ with heat absorption parameter G.

Figure 8 is plotted to display the effect of Cu-nanoparticle volume parameter ϕ_1 hybrid nanofluid velocity profiles $f'(\eta)$, while Figure 9 presented the temperature profiles $\theta(\eta)$ against the same parameters. It is obviously noted that both profiles increase when we improves the ϕ_1 from 0% to 10% due to higher nanoparticles in the fluid system that enhances the resistance and improving both boundary layer thickness at the same time. Further, Figures 10 and 11 illustrated the $f'(\eta)$ and $\theta(\eta)$, accordingly, against the effect of suction parameter S. Since the other parameters are in a constant value, we notified that the impact of S will enhances the hybrid nanofluid velocity but performs a reverse behaviour through temperature profiles $\theta(\eta)$. The reason of this pattern might be explained by demonstrating the added number of S will stabilizes the growth of boundary layer. However, the decaying pattern of thermal transmittance in Figures 11 may be elaborated by the S parameter seems to decelerate the fluid particles along the porous wall and thus retards the heat transfer broadening.

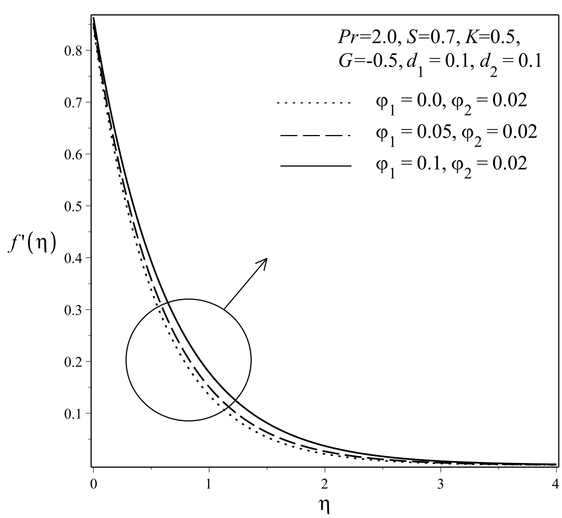

Figure 8: Velocity profiles $f'(\eta)$ with Cu-nanoparticle volume parameter ϕ_1.

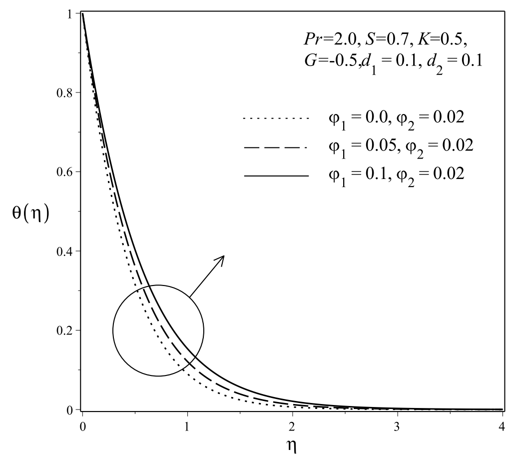

Figure 9: Temperature profiles $\theta(\eta)$ with Cu-nanoparticle volume parameter ϕ_1.

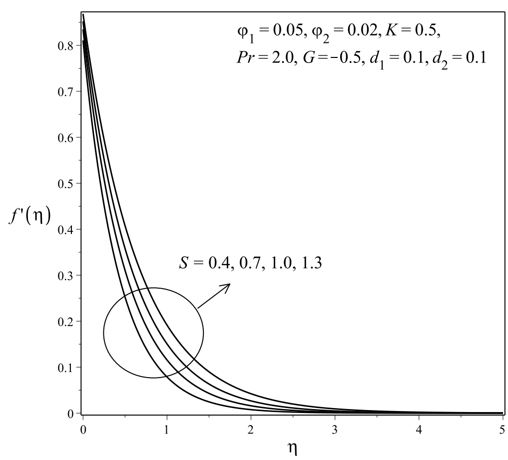

Figure 10: Velocity profiles $f'(\eta)$ with suction parameter S.

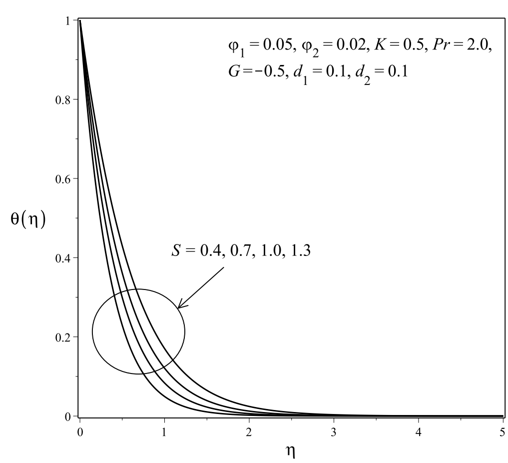

Figure 11: Temperature profiles $\theta(\eta)$ with suction parameter S.

The influence of Prandtl number *Pr* on temperature profiles $\theta(\eta)$ is depicted in Figure 12. This figure displayed the thermal boundary layer thickness to decrease against the additional numbers of *Pr*. It is noticeable that Prandtl number represents the ratio of momentum diffusivity against thermal diffusivity, where any increasing number of *Pr* corresponds the fluid to generate weaker thermal diffusivity. Hence, the thickness of thermal boundary layer in fluid flow corresponding to a large number of *Pr* is considered small and less efficient to compared with lesser amount of Prandtl number in any fluid system. Nevertheless, the importance of Prandtl number should not be underestimated as *Pr* plays a significant role in cooling process where it was used to control the thermal and momentum boundary layer thicknesses.

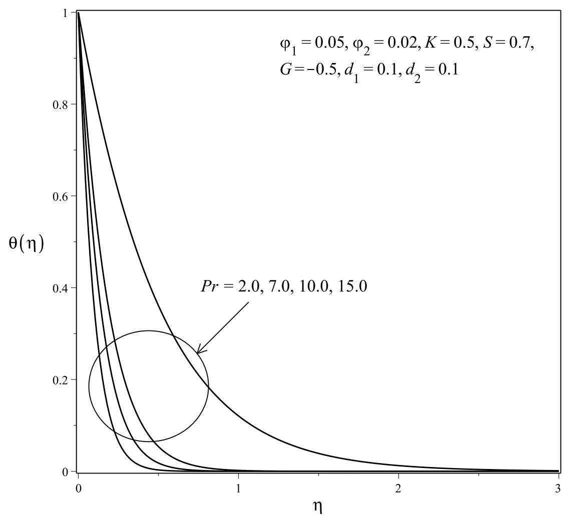

Figure 12: Temperature profiles $\theta(\eta)$ with Prandtl number *Pr*.

4 Conclusions

In this current study, we analyzed and thoroughly discussed the study of natural convection of hybrid nanofluid conjoined by Cu-Al_2O_3 nanoparticles while H_2O worked as a base fluid in a permeable non-Darcy porous medium with consideration of second-order velocity slip and internal heat absorption. The mathematical outputs were obtained by converting the respective PDEs into ODEs with a method of similarity transformation. The final outcomes throughout this work include

i) It is found that the performance of boundary layer flow reflects better with the hybrid of two distinct nanoparticles between copper (Cu) and aluminium oxide (Al_2O_3), rather than the impact of mono aluminium oxide (Al_2O_3) nanoparticle.

ii) The skin friction coefficient factor C_f and the local Nusselt number Nu_x are improving alongside the nanoparticles of hybrid nanofluid.

iii) It is monitored that volume particle parameter ϕ, porous medium permeability parameter K and suction parameter S contribute the fluid velocity of nanofluids to rise, except the second-order velocity slip parameter d_2.

iv) Volume particle parameter ϕ and heat absorption parameter G tend to enhance the rate of thermal transmittance, while a declining pattern is observed against the suction parameter S and Prandtl number Pr.

Acknowledgement This work is ostensibly supported by the Ministry of Higher Education Malaysia through the Fundamental Research Grant Scheme (FRGS). Authors also wish to appreciate the respective reviewers and editors for their fruitful comments and suggestions.

Conflicts of Interest The authors declare no conflict of interest.

References

[1] S. Abu Bakar, N. S. Wahid, N. M. Arifin & N. S. Khashiie (2022). The flow of hybrid nanofluid past a permeable shrinking sheet in a darcy–forchheimer porous medium with second-order velocity slip. *Waves in Random and Complex Media*, pp. 1–18. https://doi.org/10.1080/17455030.2021.2020375.

[2] S. A. Al-Sanea (2004). Mixed convection heat transfer along a continuously moving heated vertical plate with suction or injection. *International Journal of Heat and Mass Transfer*, *47*(6-7), 1445–1465. https://doi.org/10.1016/j.ijheatmasstransfer.2003.09.016.

[3] S. U. S. Choi & J. A. Eastman (1995). *Enhancing thermal conductivity of fluids with nanoparticles*. Argonne National Lab, United States.

[4] Y.-M. Chu, K. S. Nisar, U. Khan, H. Daei Kasmaei, M. Malaver, A. Zaib & I. Khan (2020). Mixed convection in MHD water-based molybdenum disulfide-graphene oxide hybrid nanofluid through an upright cylinder with shape factor. *Water*, *12*(6), 1723. https://doi.org/10.3390/w12061723.

[5] S. Das, R. N. Jana & O. D. Makinde (2017). MHD flow of $Cu-Al_2O_3$/water hybrid nanofluid in porous channel: Analysis of entropy generation. In *Defect and Diffusion Forum*, pp. 42–61. Scientific.Net, Switzerland.

[6] S. P. A. Devi & S. S. U. Devi (2016). Numerical investigation of hydromagnetic hybrid $Cu-Al_2O_3$/water nanofluid flow over a permeable stretching sheet with suction. *International Journal of Nonlinear Sciences and Numerical Simulation*, *17*(5), 249–257. https://doi.org/10.1515/ijnsns-2016-0037.

[7] K. Ezhil, S. K. Thavada & S. B. Ramakrishna (2020). MHD slip flow and heat transfer of $Cu-Fe_3O_4$/ethylene glycol-based hybrid nanofluid over a stretching surface. *11*(4), 11956–11968. https://doi.org/10.33263/briac114.1195611968.

[8] S. S. Ghadikolaei, M. Yassari, H. Sadeghi, K. Hosseinzadeh & D. D. Ganji (2017). Investigation on thermophysical properties of $tio2-Cu/H_2O$ hybrid nanofluid transport dependent on shape factor in MHD stagnation point flow. *Powder Technology*, *322*, 428–438. https://doi.org/10.1016/j.powtec.2017.09.006.

[9] P. Gokulavani, M. Muthtamilselvan & B. Abdalla (2021). Impact of injection/suction and entropy generation of the porous open cavity with the hybrid nanofluid. *Journal of Thermal Analysis and Calorimetry*, *147*, 1–14. https://doi.org/10.1007/s10973-021-10636-2.

[10] F. Haider, T. Hayat & A. Alsaedi (2021). Flow of hybrid nanofluid through Darcy-Forchheimer porous space with variable characteristics. *Alexandria Engineering Journal*, *60*(3), 3047–3056. https://doi.org/10.1016/j.aej.2021.01.021.

[11] Y.-H. Hung, W.-P. Wang, Y.-C. Hsu & T.-P. Teng (2017). Performance evaluation of an air-cooled heat exchange system for hybrid nanofluids. *Experimental Thermal and Fluid Science*, *81*, 43–55. https://doi.org/10.1016/j.expthermflusci.2016.10.006.

[12] W. Ibrahim (2017). Magnetohydrodynamics (MHD) flow of a tangent hyperbolic fluid with nanoparticles past a stretching sheet with second order slip and convective boundary condition. *Results in Physics*, *7*, 3723–3731. https://doi.org/10.1016/j.rinp.2017.09.041.

[13] W. Jamshed, S. U. Devi & K. S. Nisar (2021). Single phase based study of $Ag - Cu/EO$ williamson hybrid nanofluid flow over a stretching surface with shape factor. *Physica Scripta*, *96*(6), 065202. https://doi.org/10.1088/1402-4896/abecc0.

[14] W. A. Khan & I. Pop (2010). Boundary-layer flow of a nanofluid past a stretching sheet. *International Journal of Heat and Mass Transfer*, *53*(11-12), 2477–2483. https://doi.org/10.1016/j.ijheatmasstransfer.2010.01.032.

[15] L. A. Lund, Z. Omar, S. Dero, I. Khan, D. Baleanu & K. S. Nisar (2020). Magnetized flow of $Cu + Al_2O_3 + H_2O$ hybrid nanofluid in porous medium: Analysis of duality and stability. *Symmetry*, *12*(9), 1513. https://doi.org/10.3390/sym12091513.

[16] S. Manjunatha, B. A. Kuttan, S. Jayanthi, A. Chamkha & B. Gireesha (2019). Heat transfer enhancement in the boundary layer flow of hybrid nanofluids due to variable viscosity and natural convection. *Heliyon*, *5*(4), e01469. https://doi.org/10.1016/j.heliyon.2019.e01469.

[17] H.-M. Nieh, T.-P. Teng & C.-C. Yu (2014). Enhanced heat dissipation of a radiator using oxide nano-coolant. *International Journal of Thermal Sciences*, *77*, 252–261. https://doi.org/10.1016/j.ijthermalsci.2013.11.008.

[18] I. S. Oyelakin, S. Mondal & P. Sibanda (2016). Unsteady Casson nanofluid flow over a stretching sheet with thermal radiation, convective and slip boundary conditions. *Alexandria Engineering Journal*, *55*(2), 1025–1035. https://doi.org/10.1016/j.aej.2016.03.003.

[19] S. Suresh, K. P. Venkitaraj, P. Selvakumar & M. Chandrasekar (2011). Synthesis of $Al_2O_3 - Cu$/water hybrid nanofluids using two step method and its thermo physical properties. *Colloids and Surfaces A: Physicochemical and Engineering Aspects*, *388*(1-3), 41–48. https://doi.org/10.1016/j.colsurfa.2011.08.005.

[20] A. Tulu & W. Ibrahim (2021). Effects of second-order slip flow and variable viscosity on natural convection flow of $CNTs - Fe_3O_4$/water hybrid nanofluids due to stretching surface. *Mathematical Problems in Engineering*, *2021*, Article ID: 8407194. https://doi.org/10.1155/2021/8407194.

[21] M. Usman, M. Hamid, T. Zubair, R. U. Haq & W. Wang (2018). $Cu - Al_2O_3$/water hybrid nanofluid through a permeable surface in the presence of nonlinear radiation and variable thermal conductivity via lsm. *International Journal of Heat and Mass Transfer*, *126*, 1347–1356. https://doi.org/10.1016/j.colsurfa.2011.08.005.

[22] B. Venkateswarlu & P. V. Satya Narayana (2021). $Cu - Al_2O_3/H_2O$ hybrid nanofluid flow past a porous stretching sheet due to temperatue-dependent viscosity and viscous dissipation. *Heat Transfer*, *50*(1), 432–449. https://doi.org/10.1002/htj.21884.

[23] I. Waini, A. Ishak, T. Groşan & I. Pop (2020). Mixed convection of a hybrid nanofluid flow along a vertical surface embedded in a porous medium. *International Communications in Heat and Mass Transfer*, *114*, 104565. https://doi.org/10.1016/j.icheatmasstransfer.2020.104565.

[24] L. Wu (2008). A slip model for rarefied gas flows at arbitrary Knudsen number. *Applied Physics Letters*, *93*(25), 253103. https://doi.org/10.1063/1.3052923.

[25] L. Yan, S. Dero, I. Khan, I. A. Mari, D. Baleanu, K. S. Nisar, E.-S. M. Sherif & H. S. Abdo (2020). Dual solutions and stability analysis of magnetized hybrid nanofluid with joule heating and multiple slip conditions. *Processes*, *8*(3), 332. https://doi.org/10.3390/pr8030332.

[26] U. Yashkun, K. Zaimi, N. A. A. Bakar, A. Ishak & I. Pop (2020). MHD hybrid nanofluid flow over a permeable stretching/shrinking sheet with thermal radiation effect. *International Journal of Numerical Methods for Heat & Fluid Flow*, *31*(3), 1014–1031. https://doi.org/10.1108/HFF-02-2020-0083.